AIAA SciTech Forum
23-27 January 2023, National Harbor, MD & Online
AIAA SCITECH 2023 Forum

10.2514/6.2023-0167

CARS in an Inductively Coupled Plasma Torch, Part 1: High Temperature Nitrogen Thermometry

Dan Fries*, Spenser T. Stark†, John S. Murray‡, Noel Clemens§, and Philip L. Varghese¶
Dept. of Aerospace Engineering and Engineering Mechanics, University of Texas, Austin, TX 78712, USA

Rajkumar Bhakta‖, Elijah R. Jans**, and Sean Kearney††
Engineering Sciences Center, Sandia National Laboratories, Albuquerque, NM 87123, USA

The current interest in hypersonic flows and the growing importance of plasma applications necessitate the development of diagnostics for high-enthalpy flow environments. Reliable and novel experimental data at relevant conditions will drive engineering and modeling efforts forward significantly. This study demonstrates the usage of nanosecond Coherent Anti-Stokes Raman Scattering (CARS) to measure temperature in an atmospheric, high-temperature (> 5500 K) air plasma. The experimental configuration is of interest as the plasma is close to thermodynamic equilibrium and the setup is a test-bed for heat shield materials. The determination of the non-resonant background at such high-temperatures is explored and rotational-vibrational equilibrium temperatures of the N_2 ground state are determined via fits of the theory to measured spectra. Results show that the accuracy of the temperature measurements is affected by slow periodic variations in the plasma, causing sampling error. Moreover, depending on the experimental configuration, the measurements can be affected by two-beam interaction, which causes a bias towards lower temperatures, and stimulated Raman pumping, which causes a bias towards higher temperatures. The successful demonstration of CARS at the present conditions, and the exploration of its sensitivities, paves the way towards more complex measurements, e.g. close to interfaces in high-enthalpy plasma flows.

I. Introduction

Experimental measurements in high-enthalpy flows are of large interest for hypersonics and plasma research. They yield new insights and drive engineering developments for supersonic aircraft, re-entry technology, material processing, and electromagnetic propulsion technologies. However, measurements in representative environments are challenging due to high temperatures, strong background luminescence, possible thermodynamic non-equilibrium, and the presence of multiple chemically active species.

Coherent Anti-Stokes Raman Scattering (CARS) has been used extensively for temperature and species measurements in combustion environments [1]. It has also been used to detect multiple species simultaneously [2, 3], characterize non-equilibrium states [4], and attempts have been made to extend the diagnostic to temperatures exceeding 5000 K [5–8]. Thus, it will be a useful tool for measurements in the aforementioned high-enthalpy flow environments.

In this paper, we demonstrate multiplex nanosecond CARS [9] measurements in the plume of an inductively coupled plasma (ICP) torch running on dry air. We determine the N_2 ground state rotational-vibrational equilibrium temperature and find peak values above 6000 K. We analyze the expected non-resonant susceptibility, report high quality single shot temperature measurement capabilities, and explore possible sources of uncertainty. Leveraging this demonstration, we are also performing temperature and multi-species measurements near the surface of a graphite sample exposed to the plasma plume. First results of these efforts are presented in the companion paper by Kearney *et al.* [10].

*Postdoctoral Researcher, Dept. of Aerospace Engineering and Engineering Mechanics, dan.fries@austin.utexas.edu, AIAA Member.
†Graduate Student, AIAA Member.
‡Graduate Student, AIAA Member.
§Professor, Dept. of Aerospace Engineering and Engineering Mechanics, clemens@mail.utexas.edu, AIAA Fellow.
¶Professor, Dept. of Aerospace Engineering and Engineering Mechanics, varghese@mail.utexas.edu, AIAA Associate Fellow.
‖Senior Engineering and Operations Staff, AIAA Member.
**Postdoctoral Appointee, Engineering Sciences Center, AIAA Member.
††Distinguished Member of the Technical Staff, Associate Fellow AIAA.

II. Methodology

The ICP torch facility at UT Austin, in the Flowfield Imaging Laboratory, is shown during operation with air in Fig. 1a. The operation set-point is controlled via adjustment of the direct current (DC) anode voltage on the triode circuit, from 9-12 kV, and the maximum DC input power is 50 kW. The triode and tank circuit produce radio-frequency (RF) alternating current at a frequency of 6 MHz, which powers the magnetic field sustaining the plasma. An annotated schematic of the torch body is presented in Fig. 1b. The body has a length of 250 mm and the outlet nozzle has a diameter of 30 mm. In this study, only air is used as the working gas (Linde AI 0.0UZ). A detailed general characterization of the ICP torch has been presented previously in [11]. All data in the present paper has been taken with an air flow rate of 30 slpm and a DC anode voltage of 10 kV, i.e. a plasma power of $\sim$ 10.6 kW.

(a) ICP torch facility with power supply and sample holding arms.

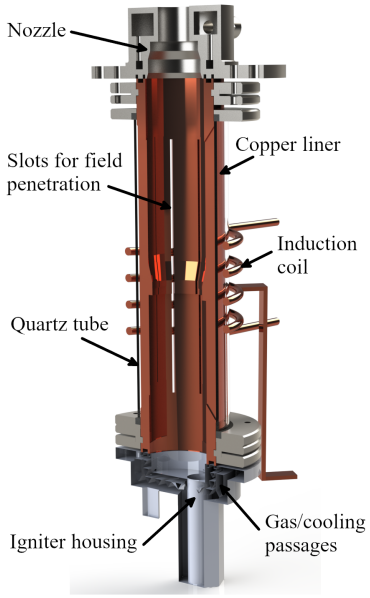

(b) ICP torch body schematic.

Fig. 1 Overview of the ICP torch setup.

Measurements of the ro-vibrational equilibrium temperature are made using a multiplex nanosecond CARS system. Thus, the entire N_2 CARS spectrum can be recorded in one laser shot. The experimental setup is shown schematically in Fig. 2a, and the corresponding transition diagram in Fig. 2b. The broadband dye laser acts as the Stokes beam and its spectral profile is centered at 607 nm with a full-width at half-maximum (FWHM) of 160 cm^{-1}. The two pump beams are degenerate, both being emitted by a Coherent Powerlite 9010 Nd:YAG laser at the second harmonic wavelength, i.e. 532 nm, at 10 Hz. For phase matching, the three beams are arranged in a BOXCARS configuration [9].

From previous emission spectroscopy and spontaneous Raman scattering measurements [11, 12], we expect the plume center temperature, close to the nozzle exit, to be in the range of 5000-7000 K. At such high temperatures, the higher lying vibrational and rotational states are significantly populated, leading to a drop in the CARS signal intensity of individual transitions and resulting in complex CARS spectra. That signal levels should drop with increasing temperature can be discerned from the expression given in [9] for the CARS resonant susceptibility. At high temperatures, the upper state populations increase while lower lying states are less populated. This reduces the population difference between the two states probed with CARS, N_a and N_b, reducing the magnitude of the CARS signal for this state pair:

$$\chi_{CARS} = \frac{8\pi^2 n_1 \epsilon_0 c^4 (N_a - N_b)\left(\frac{\partial\sigma}{\partial\Omega}\right)}{n_2 \hbar \omega_2^4 \left(\omega_{ba} - \omega_1 + \omega_2 - i\frac{\Gamma_{ab}}{2}\right)}. \tag{1}$$

Here, ϵ_0 is the vacuum permittivity, c is the speed of light, $\partial\sigma/\partial\Omega$ is the differential Raman cross section, $n1$ and n_2

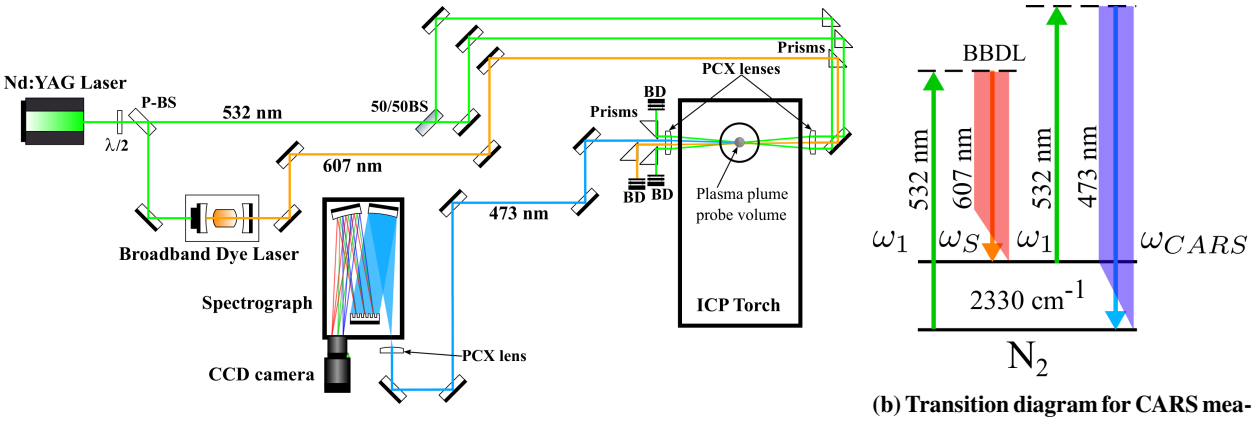

(a) Multiplex nanosecond CARS setup used on the ICP torch.

(b) Transition diagram for CARS measurements of nitrogen.

Fig. 2 Overview of the CARS setup.

are the indices of refraction of the media the pump and Stokes beam are propagating in, respectively, $\hbar$ is the reduced Planck constant, ω_1 and ω_2 are the frequencies of the pump and Stokes laser, ω_{ba} is the Raman resonance between states a and b, and Γ_{ab} is the lifetime of the Raman transition.

An additional challenge is the high background luminosity of the plasma. To tackle both the signal strength and background luminosity issues, we use an intensified Princeton Instruments PI-MAX 4 1024i camera, set to a gating time of 50 ns. This rejects all of the natural plasma radiation. The relative gain of the camera is set between 1.0-74.9 in the presented data sets, providing sufficient signal levels even in the hottest part of the ICP plasma plume and more dynamic range in the colder mixing regions. Before being recorded by the intensified CCD camera, the CARS signal from the N_2 Q-branch near 473 nm is spectrally dispersed in a Princeton Instruments Spectra Pro HRS-750 spectrometer with a 1800 g/mm grating, yielding a dispersion of 0.35 cm^{-1}/pixel and a spectral resolution of $\sim$ 1 cm^{-1}.

The recorded CARS spectra are wavenumber calibrated by comparison with theoretical spectra from CARSFT [13], background subtracted, and intensity corrected with the non-resonant signal measured in pure argon. To obtain temperatures, the spectra are curve-fitted to a library of CARSFT spectra. The theoretical spectra are generated assuming isolated lines and only collision-broadening is currently considered, neglecting any other effects that might become relevant at the high ICP torch temperatures. The self-broadened N_2 linewidths are calculated with the modified-exponential-gap model. Finally, the CARS susceptibility is convolved with a Gaussian instrument function. The constants used in the modified-exponential-gap model were determined at a maximum temperature of 2400 K [14], but our approach extrapolates the Raman linewidths to much higher temperatures. Both the temperature and the non-resonant background susceptibility are fitted simultaneously. The non-resonant background contribution can change, as the composition of the plume can vary significantly from high- to lower-temperature regions. Thus, it is also desirable to estimate the expected non-resonant susceptibility, χ_{nr} a priori for a sanity check, as temperature and χ_{nr} are correlated.

To illustrate changes in the non-resonant background susceptibility, we approximate χ_{nr} accounting for N_2 [15], O_2 [16], and NO [17], calculating equilibrium compositions of air using NASA CEA [18]. The total non-resonant susceptibility is calculated as $\chi_{nr} = \sum_i X_i \chi_{nr,i}$, for a given temperature. Unfortunately, no susceptibility values for atomic oxygen and nitrogen are found in the literature. Since oxygen and nitrogen are in the same period as neon, it might be reasonable to assume that their non-resonant susceptibility is approximately a factor 10 smaller than that of N_2 and O_2 [17]. In that case, Fig. 3 shows that the non-resonant background susceptibility correlates almost linearly with the nitrogen mole fraction over the expected range of temperatures. If the susceptibilities of O and N atoms approach their molecular counterparts, Fig. 3 shows that χ_{nr} stays pretty much constant over the entire range of temperatures. Finally, if the susceptibilities of O and N grow larger, the non-resonant susceptibility would actually increase compared to room temperature air. Further research is required to produce a reliable bound on the non-resonant susceptibility in the high-temperature ICP plasma.

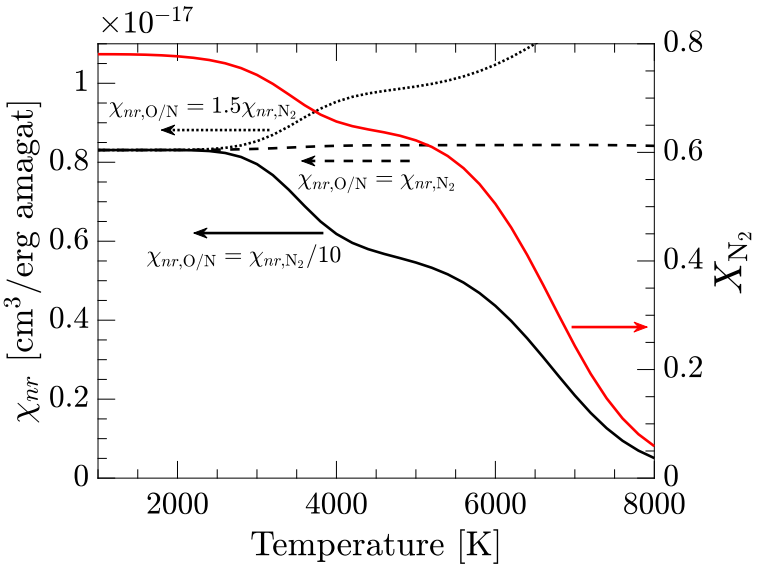

Fig. 3 Estimate of the non-resonant susceptibility of the background gas and of the nitrogen equilibrium mole fraction, over the expected range of temperatures in the present experiment.

III. Results

Representative examples of a fit to an averaged CARS spectrum, to a ten shot average, and to a single shot are shown in Fig. 4. The average spectrum is calculated over 500 single shots taken at 10 Hz and the corresponding fit is accurate, with the higher lying vibrational and rotational states being clearly distinguishable. The ten shot average corresponds to one second of measurement time and the residual is only slightly more noisy. The single shot spectrum is significantly more noisy but still shows agreement with the theoretical trends. The measurements are taken with the following beam pulse energies: 28.0 mJ/pulse and 32.0 mJ/pulse in the pump beams, and 19.0 mJ/pulse in the Stokes beam.

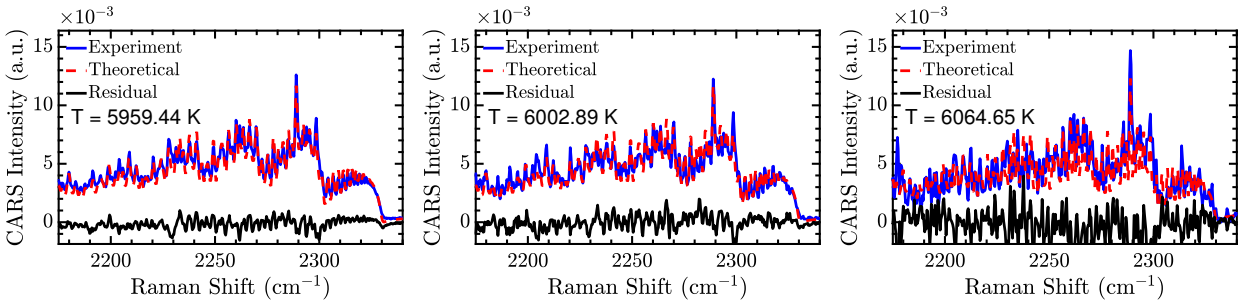

(a) Average Spectrum. **(b) Ten shot average spectrum.** **(c) Single shot spectrum.**

Fig. 4 Example spectra and CARSFT fits for measurements taken on the centerline. The average spectrum is the mean of 500 single shots, taken 6 mm above the ICP torch nozzle, with a relative gain setting of 74.9 using two f = 300 mm convex lenses to form the measurement volume. The single shot spectrum is a representative example from this data set.

The measured temperature distribution along the torch centerline, above the nozzle, is shown in Fig. 5a, taken with 28.0 mJ/pulse and 32.0 mJ/pulse in the pump beams, and 19.0 mJ/pulse in the Stokes beam. Each data point corresponds to the average of 10 measurements with an accumulation of 10 shots each.The quoted probe measurement volume length has been determined by scanning a 150 µm thick microscope glass slide along the laser beams, while measuring the non-resonant signal generated in the process. The probe volume is defined as the range over which 5-95% of the integrated CARS signal is generated. Some of the data points exhibit a larger spatial variation than expected from previous measurements [11] and from the generally smooth average temperature variation in a hot plume.

Preliminary calculations have shown that the unexpected variations are not due to spatial averaging. Spatial

averaging can be observed in the presence of large gradients over the finite length of a probe volume [19]. Due to the non-linear dependence of the CARS signal on population density, see Eq. (1), the presence of colder gases contributes disproportionately to the resulting CARS spectrum. Thus, biasing the result non-linearly towards lower temperatures, even during a single shot measurement. However, the gradients in the ICP torch plume are not large enough to explain jumps on the order of 1000 K. An analysis of the time series of single shot measurements and additional measurements, presented later in this paper, suggest other sources of errors.

Radial temperature distributions are shown in Fig. 5b, taken with 28.0 mJ/pulse and 32.0 mJ/pulse in the pump beams, and 19.0 mJ/pulse in the Stokes beam. Measurements were taken 6 mm above the nozzle. One data set is for a longer measurement volume (f = 500 mm focusing lenses) and an average of 50 measurements with an accumulation of 10 shots each; the second data set is for a shorter measurement volume (f = 300 mm focusing lenses) and 500 single shot measurements.

An outstanding feature of the results in Fig. 5b is, that the peak temperature measured with the smaller measurement volume is almost 60% higher than measured with the larger measurement volume. It is unlikely that the previously mentioned spatial averaging is responsible for such a large temperature difference, as the gradients are not that strong. Other possibilities are sampling errors, two-beam interaction, and stimulated Raman pumping. We will first discuss possible sampling errors, which are also relevant for the aforementioned spatial temperature variations in the axial temperature profiles.

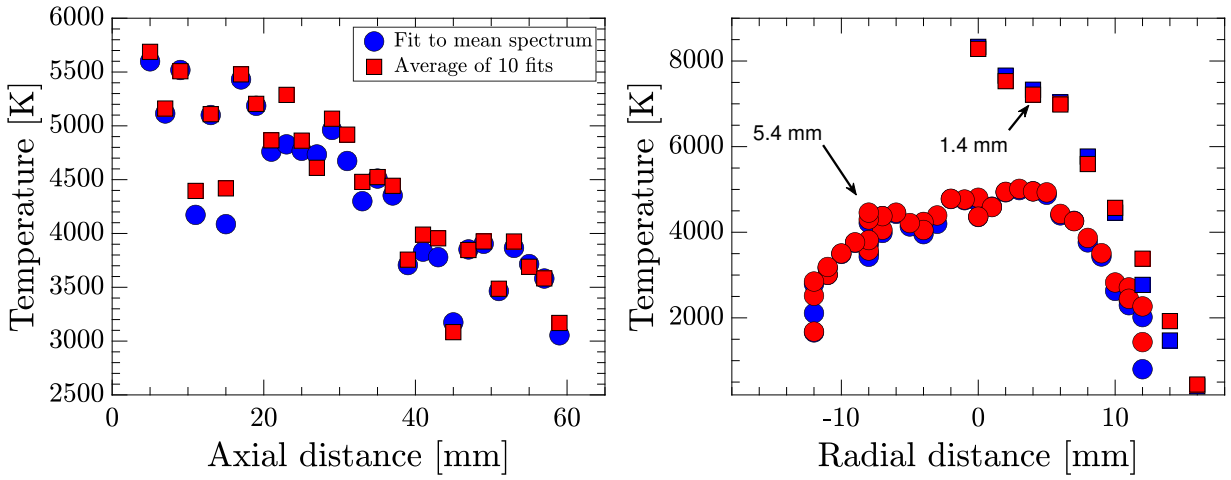

(a) Temperature as a function of axial distance measured above the ICP torch nozzle. The CARS probe volume length is 4.8 mm, formed with two f = 500 mm convex lenses. Individual spectra are really 10 accumulations.

(b) Temperature as a function of radial distance measured 6 mm above the nozzle. The probe volume length is annotated to each data set. The longer measurement volume data points consist of 100 single shots; the smaller measurement volume data points of 500 single shots.

Fig. 5 Axial and radial CARS temperature distributions. The edges of the nozzle are at ±15 mm. Blue markers indicate temperatures derived from mean spectra, red markers indicate the mean temperature of fits to single shot data.

The time series for the axial and radial data in Fig. 6a and Fig. 6b, respectively, show that there are time periodic variations in the plasma properties. The period of the variations appears to be on the order of ~ 20 s and becomes more pronounced towards the edge of the nozzle; compare the data taken at 0 mm and 8 mm distance from the centerline in Fig. 6b. The variations in Fig. 6a are large enough and have a long enough period to explain some of the spatial temperature jumps in the axial measurements, Fig. 5a, and radial measurements in Fig. 5b. Thus, sampling error is responsible for at least part of the temperature jumps observed, when data series are not long enough to average over multiple periods of the observed temperature variations. The larger temperature variations closer to the edge of the nozzle will have a stronger effect. However, the observed time dependence cannot explain the 60% temperature difference between the large and small measurement volume cases in Fig. 5b. On the centerline, the maximum temperature variation does not exceed ~ 1500 K. The peak temperature variation 8 mm from the centerline, in Fig. 6b, is ~ 2800 K.

A repetition of the radial measurements with the f = 300 mm lenses revealed that the presented results in Fig. 5a and Fig. 5b are not only affected by sampling error, but also by a two-beam interaction (in the case of the f = 500 mm

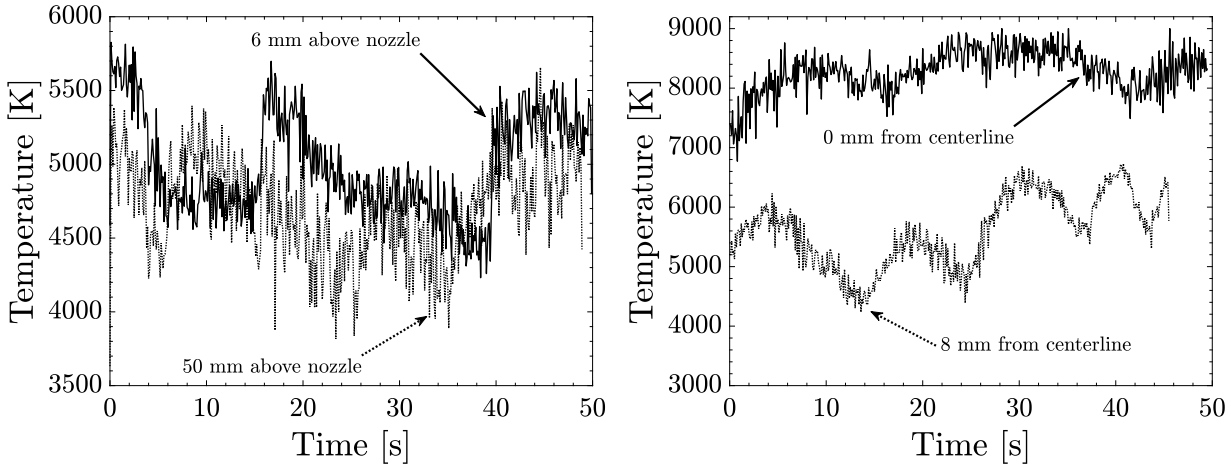

(a) Data points from measurements on the centerline, 500 single shots.

(b) Data points from measurements in the radial direction, 6 mm above the nozzle, 500 single shots.

Fig. 6 Temperature time histories computed from single shot data. 500 single shots over a 50 s observation time.

lenses) and stimulated Raman pumping (in the case of the $f = 300$ mm lenses). The two-beam interaction causes a bias towards lower temperatures. It is caused by one of the pump beams individually interacting with the Stokes beam to achieve a four-wave mixing process, generating a CARS signal that, due to phase matching requirements, is collinear with the respective pump beam. In our setup, the Stokes beam has a significantly larger diameter than the pump beams and is focusing more poorly. Thus, the two-beam interaction occurs beyond the nominally determined probe volume length in colder gas regions and biases the recorded spectrum towards the lower temperature signal. We confirmed this using a DataRay WinCamD-LCM beam profiler and a corresponding measurement is shown in Fig. 7a. It cam be seen that, conceptually, the beam labelled as “Pump 1" can interact with the defocusing Stokes beam significantly beyond the nominal CARS volume. When using the $f = 300$ mm lenses, we increase the crossing angle and the resulting measurements are less affected by the two-beam interaction.

The two-beam interaction becomes especially relevant at the extremely high temperatures measured in the center of our plasma plume. The CARS signal here is significantly weaker than, e.g., in a flame. Thus, while it may not play a role in flame measurements, even a weak two-beam signal generated in colder gas due to beam imperfections will be noticeable here. The two-beam signal will be affected by gain on the intensified camera and can distort the hot signal noticeably. This effect is illustrated in Fig. 7b, where multiple background and intensity corrected CARS measurements are shown, taken on the centerline of the plasma plume 6 mm above the nozzle. The CARS spectra are normalized by their corresponding gain setting. The CARS + 2-beam signal was measured with the same setup used to produce the data in Fig. 5a and Fig. 5b, the 2 beam signal was isolated by blocking the central part of the presumed CARS signal beam location, and the pure CARS signal was recovered by improving the Stokes beam quality with a spatial mask and a telescope in front of the amplifier cell in the dye laser. The 2-beam signal is weak, as can be discerned from the increased gain needed to visualize it, and it looks much colder than the full CARS measurements. However, even though it is weak, it clearly distorts the nominal CARS signal and the change in the vibrational $v1 \rightarrow 0$ bandhead will yield lower temperatures when fitting spectra, as suggested by the temperatures indicated in the figure.

Nonetheless, even with two-beam interaction effects lowering the temperature in the $f = 500$ mm lens case, the 8000 K measured with the $f = 300$ mm lenses is extreme and not expected from previous measurements with emission spectroscopy and Raman scattering. The reason for these extreme temperatures is the tighter focus of the CARS beams, producing higher optical (electric) field strengths (because we kept the laser pulse energy constant) and resulting in stimulated Raman pumping (SRP) and hotter-looking vibrational bands [20, 21]. We are able to discern this effect at room temperature if enough gain is applied to our camera, saturating the $v1 \rightarrow 0$ band but exposing a population in the higher lying vibrational bands that should not be present, see Fig. 7c. This effect becomes even more severe with lower densities [20, 21], due to the lower collision frequency ($\nu_{coll} \propto n^{3/2}$), which explains why the temperature disagreement is largest at the center of the plume in Fig. 5b.

The radial temperature profile measurement was repeated with the $f = 300$ mm lenses, lower laser pulse energies, and with an improved Stokes beam profile using spatial masking and the aforementioned telescope ahead of the amplifier

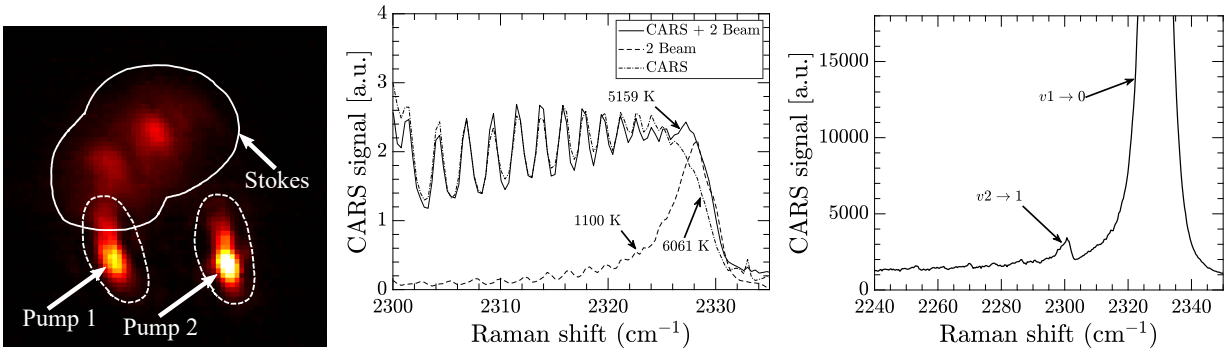

(a) Beam image 7.6 mm **ahead of the nominal beam crossing. The stokes beam is defocusing more severely than the pump beams.**

(b) Gain normalized data illustrating the effect of two-beam interaction on recorded CARS spectra. Gain settings are CARS + 2 Beam: 19.0, 2 Beam: 67.9, CARS: 52.9.

(c) Raw CARS signal count illustrating the effect of SRP. Taken at a relative gain of 9.7 in ambient air at 300 K **and 1** atm**.**

Fig. 7 Additional data showing the origin and effect of the two-beam CARS signal and SRP. All spectra are averaged from 50 measurements, each consisting of an accumulation of 10 shots, taken with 28.0 mJ/pulse **and 32.0** mJ/pulse **in the pump beams, and 19.0** mJ/pulse **in the Stokes beam. The probe volume is formed with 500** mm **focal length convex lenses.**

cell in the dye laser. In Fig. 8, each data point of the repeated measurement consists of 500 single shots and the pump and Stokes beam energies are 13.0, 21.5, and 12.5 mJ, respectively. The large number of single shots mitigates the sampling error, the lower laser pulse energy removes the effects of stimulated Raman pumping, and improving the Stokes beam quality removes the cold two-beam signal. The resulting average temperature profile is smoother than those presented in Fig. 5b and peak temperatures lie in between the previous two measurements. The temperature drops nearly monotonically from the center of the plume towards the edge, as one would expect for a hot round jet. Temperatures between all measurements agree better towards the edge of the plasma plume, where the CARS signal strength and the density are higher and, thus, any potential two-beam signal or SRP contribution is reduced. As in the other measurements, temperatures of average spectra are biased towards lower temperatures, especially at the edge of the plume where more mixing with cold ambient air occurs.

Unfortunately, these results demonstrate that it is hard to determine whether a CARS measurement is affected by a two-beam signal or SRP a priori. In general, higher gas temperatures (lower densities and lower CARS signal) and faster probe volume lenses (higher optical field strength) increase the risk of these phenomena having a noticeable effect. The beam overlap and quality can be scrutinized to determine whether a CARS signal could be generated outside of the nominal CARS volume through two-beam interaction. The central part of the CARS signal can be blocked and the gain increased, to see whether a colder than expected signal remains. Then, improving the Stokes beam quality and/or masking part of the beam will help mitigate potential two-beam signals. It should be noted that changes to the Stokes beam in this fashion will influence its spectral content, and care has to be taken that resulting CARS spectra are corrected with the appropriate non-resonant intensity signal. To identify SRP, measurements in ambient air can performed with high camera gain, to see whether higher lying vibrational bands are populated when they should not be. Subsequently, the pump and/or Stokes pulse energy can be lowered until the higher lying bands disappear from the measurement. Finally, if the power densities of the utilized laser beams as well as the Stokes beam spectral profile is known, a comparison between the laser pulse duration and the rate of molecular promotion can be made, to estimate a laser pulse energy threshold at which SRP will occur [21].

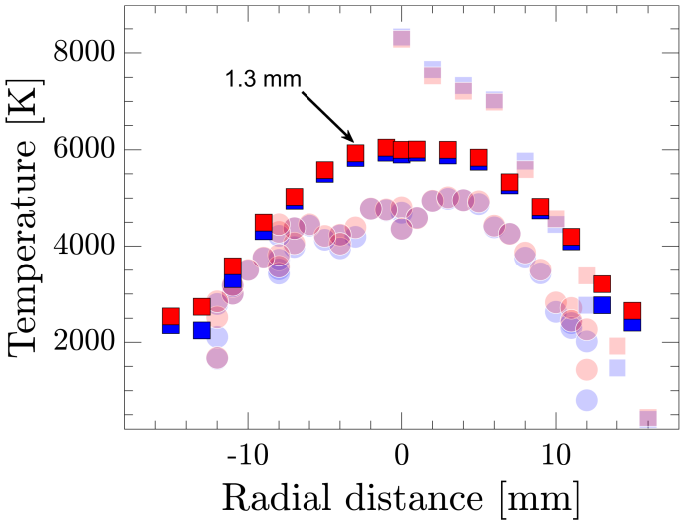

Fig. 8 Radial temperature distribution in the plasma plume, 6 mm above the exit. The measurements repeated with the f = 300 mm lenses are shown in saturated colors, the data from 5b are shown as faded symbols. Blue markers indicate temperatures derived from mean spectra, red markers indicate the mean temperature of fits to single shot data.

IV. Conclusions

Average and single-shot nitrogen CARS measurements have been performed in the plume of an ICP torch. Temperatures derived from spectral fits are in the range of 2000 to 6000 K, depending on the measurement position in the plume. A simple estimate of high temperature non-resonant susceptibilities is presented, highlighting the need for reliable third-order susceptibility data for atomic nitrogen and oxygen. Major sources of uncertainty in the measurements presented are sampling errors, due to periodic variations in plasma plume temperature, two-beam signal generation, due to Stokes beam quality and size, and stimulated Raman pumping, due to low densities and high optical field strength. Especially in the hottest part of the plasma plume, the two-beam signal and the stimulated Raman pumping become a bigger problem because the nominal CARS signal strength is lower and collision frequencies decrease. The identification of these unwanted effects has been discussed and measurements have been presented that employ mitigation strategies, resulting in reasonable temperatures (compared to results from other measurement methodologies) and a more well behaved radial temperature profile. Future work will address the contribution of atomic species to the non-resonant susceptibility and quantify uncertainties, accuracy, and precision in more detail. The utilization of a spatial filter on the Stokes beam and/or the CARS signal beam will be explored as a means to mitigate the two-beam signal generation. Finally, a companion paper [10] reports on simultaneous N_2 and CO CARS spectra taken near a graphite sample in the plasma plume of the ICP torch.

Acknowledgments

This work was funded by the United States Department of Energy (DOE) and its National Nuclear Security Administration (NNSA). University of Texas personnel are supported by the Department of Energy, National Nuclear Security Administration under Award Number DE-NA0003969.

Sandia National Laboratories personnel were supported by DOE/NNSA Science Campaign-6 funding. Sandia National Laboratories is a multimission laboratory managed and operated by the National Technology and Engineering Solutions of Sandia, LLC, a wholly owned subsidiary of Honeywell International, Inc., for the U.S. Department of Energy's National Nuclear Security Administration under Contract No. DE-NA0003525.

References

[1] Roy, S., Gord, J. R., and Patnaik, A. K., "Recent advances in coherent anti-Stokes Raman scattering spectroscopy: Fundamental developments and applications in reacting flows," *Pro. Energy Comb. Sci.*, Vol. 36, No. 2, 2010, pp. 280–306.

[2] Gallo, E., Cantu, L., Cutler, A. D., Rahimi, M. J., and Chelliah, H. K., "WIDECARS measurements of major species concentration and temperature in an air-ethylene flame," *30th AIAA Aerodynamic Measurement Technology and Ground Testing Conference*, AIAA 2014-2525, Atlanta, GA, 2014, pp. 1–18.

[3] Rock, N., Hsu, P. S., Lauriola, D., Rahman, N., Estevadeordal, J., Grib, S. W., Jiang, N., Kearney, S. P., and Wrzesinski, P., "WIDECARS multi-parameter measurements in premixed ethylene–air flames using a wavelength stable ultrabroadband dye laser," *Appl. Optics*, Vol. 59, No. 8, 2020, pp. 2649–2655.

[4] Lempert, W. R., and Adamovich, I. V., "Coherent anti-Stokes Raman scattering and spontaneous Raman scattering diagnostics of nonequilibrium plasmas and flows," *J. Phys. D: Appl. Phys.*, Vol. 47, No. 43, 2014, p. 433001.

[5] Bornemann, T., Kornas, V., Schulz-von der Gathen, V., and Döbele, H., "Temperature and concentration measurements of molecular hydrogen in a filamentary discharge by coherent anti-Stokes Raman spectroscopy (CARS)," *Appl. Phys. B - Lasers O.*, Vol. 51, No. 5, 1990, pp. 307–313.

[6] Grisch, F., Bouchardy, P., Joly, V., Marmignon, C., Koch, U., and Gulhan, A., "Coherent anti-Stokes Raman scattering measurements and computational modeling of nonequilibrium flow," *AIAA J.*, Vol. 38, No. 9, 2000, pp. 1669–1675.

[7] Dedic, C. E., Meyer, T. R., and Michael, J. B., "Single-shot ultrafast coherent anti-Stokes Raman scattering of vibrational/rotational nonequilibrium," *Optica*, Vol. 4, No. 5, 2017, pp. 563–570.

[8] Gülhan, A., Esser, B., Koch, U., Fischer, M., Magens, E., and Hannemann, V., "Characterization of high-enthalpy-flow environment for ablation material tests using advanced diagnostics," *AIAA J.*, Vol. 56, No. 3, 2018, pp. 1072–1084.

[9] Eckbreth, A. C., *Laser diagnostics for combustion temperature and species*, Vol. 3, CRC press, 1996.

[10] Kearney, S. P., Bhakta, R. B., Fries, D., Murray, J. S., Stark, S. T., Clemens, N. T., and Varghese, P. L., "CARS in an Inductively Coupled Plasma Torch, Part 2: Temperature and Carbon-Monoxide Measurements in the Reaction Layer of a Graphite Ablator," *AIAA SciTech 2023 Forum*, AIAA, National Harbor, MD, 2023, pp. 1–5.

[11] Greene, B. R., Clemens, N. T., Varghese, P. L., Bouslog, S., and Del Papa, S. V., "Characterization of a 50kW Inductively Coupled Plasma Torch for Testing of Ablative Thermal Protection Materials," *55th AIAA Aerospace Sciences Meeting*, AIAA 2017-0394, Grapevine, TX, 2017, pp. 1–14.

[12] Fries, D., Clemens, N. T., and Varghese, P., "Time Dynamics of an Inductively Coupled Plasma Torch," *AIAA SciTech 2022 Forum*, AIAA 2022-0984, San Diego, CA, 2022, pp. 1–13.

[13] Palmer, R. E., "The CARSFT computer code calculating coherent anti-Stokes Raman spectra: User and programmer information," Tech. rep., Sandia National Lab.(SNL-CA), Livermore, CA (United States), 1989.

[14] Lavorel, B., Guillot, L., Bonamy, J., and Robert, D., "Collisional Raman linewidths of nitrogen at high temperature (1700–2400 K)," *Opt. Lett.*, Vol. 20, No. 10, 1995, pp. 1189–1191.

[15] Farrow, R. L., Lucht, R. P., and Rahn, L. A., "Measurements of the nonresonant third-order susceptibilities of gases using coherent anti-Stokes Raman spectroscopy," *J. Opt. Soc. Am. B*, Vol. 4, No. 8, 1987, pp. 1241–1246.

[16] Hahn, J. W., and Lee, E. S., "Measurement of nonresonant third-order susceptibilities of various gases by the nonlinear interferometric technique," *J. Opt. Soc. Am. B*, Vol. 12, No. 6, 1995, pp. 1021–1027.

[17] Lundeen, T., Hou, S.-Y., and Nibler, J. W., "Nonresonant third order susceptibilities for various gases," *J. Chem. Phys.*, Vol. 79, No. 12, 1983, pp. 6301–6305.

[18] Gordon, S., and McBride, B. J., "Computer Program for Calculation of Complex Chemical Equilibrium Compositions and Applications," NASA Reference Publication 1311, 1996.

[19] Garman, J. D., and Dunn-Rankin, D., "Spatial averaging effects in CARS thermometry of a nonpremixed flame," *Comb. Flame*, Vol. 115, No. 4, 1998, pp. 481–486.

[20] Gierulski, A., Noda, M., Yamamoto, T., Marowsky, G., and Slenczka, A., "Pump-induced population changes in broadband coherent anti-Stokes Raman scattering," *Opt. Lett.*, Vol. 12, No. 8, 1987, pp. 608–610.

[21] Woodmansee, M. A., Lucht, R. P., and Dutton, J. C., "Stark Broadening and Stimulated Raman Pumping in High-Resolution N Coherent Anti-Stokes Raman Scattering Spectra," *AIAA J.*, Vol. 40, No. 6, 2002, pp. 1078–1086.